Sheffield Hallam University

Influence of nanomaterials on properties of lime and hemp/lime composites for energy efficient wall design

O'FLAHERTY, Fin <http://orcid.org/0000-0003-3121-0492>, KHALAF, Faraj Jabber and STARINIERI, Vincenzo <http://orcid.org/0000-0002-7556-0702>

Available from Sheffield Hallam University Research Archive (SHURA) at:

http://shura.shu.ac.uk/24106/

Published version

O'FLAHERTY, Fin, KHALAF, Faraj Jabber and STARINIERI, Vincenzo (2019). Influence of nanomaterials on properties of lime and hemp/lime composites for energy efficient wall design. Advances in building energy research.

Copyright and re-use policy

Influence of nanomaterials on properties of lime and hemp/lime composites for energy efficient wall design

O'Flaherty, F.J.[a]*, Khalaf, F.J[b]., Starinieri, V[c].

Centre for Infrastructure Management, Materials and Engineering Research Institute,

Sheffield Hallam University, Howard Street, Sheffield, S1 1WB, UK

*Corresponding Author: f.j.oflaherty@shu.ac.uk; Tel.: +44-114-225-3178.

Orcid IDs: [a]0000-0003-3121-0492; [b]0000-0002-5643-8437; [c]0000-0002-7556-0702.

Influence of nanomaterials on properties of lime and hemp/lime composites for energy efficient wall design

Abstract

A mixture of thermal, porosity and compressive strength properties of lime based materials were determined after adding different percentages of nanomaterials to enhance performance ($nSiO_2$, nClay and nZnO). Specimens were formulated for use in the design of a five layer energy efficient wall. Materials consisted of lime nanocomposites (used as 'Renders', properties determined were thermal conductivity (λ) and porosity) and lime/hemp shiv nanocomposites for thermal isolation ('Insulators', λ). A lime/hemp fibre nanocomposite, with PVAc glue for strength, was developed as a load bearing material ('Core', λ, strength). A solvent exchange method for drying the specimens was applied as soon as practically possible to investigate if rapid drying could be considered without adverse effects. Results showed that the maximum 28 day decrease in λ for the Render was by using 4% nZnO, λ being -18% compared to the control sample. The same render also exhibited the lowest density. For the Insulator, λ was -31% when also using 4% nZnO in comparison to the nanofree specimen. Strength of the Core exceeded 10 MPa, much greater than the minimum load bearing requirement. The paper concludes by comparing the U value of a wall utilising these findings to those from an existing lime/hemp design.

1 Introduction

Recent statistic show that energy consumption in the domestic sector in the United Kingdom (UK) in 2017 was 30 per cent of all energy consumed, exceeding the energy demand in the industrial and service sectors [BEIS, 2018]. Space heating alone for domestic buildings was 19% of the total energy consumed. Domestic energy use in the UK is a major contributor of greenhouse gas emissions, especially carbon dioxide (CO_2), not least due to the fact that properties are very energy inefficient due to their age [BRE, 2015]. Reducing energy consumption in homes is an important part of achieving the UK Government's legally binding commitment to reducing greenhouse gas emissions by at least 80% (relative to 1990 levels) by 2050 [Committee on Climate Change, 2008]. Construction of buildings in the UK is traditionally done using common building materials such as concrete blocks, bricks and less so, timber. Although timber is a sustainable product, concrete blocks and bricks require a lot of energy input during fabrication, concrete especially being a large producer of CO_2 during its manufacture. However, other low embodied energy materials are being developed and used more frequently, some are new innovations, such as alkali activated [Mangat & Ojedokun, 2018], others are a mixture of old and new such as lime and hemp composites [Collet & Prétot, 2014, Walker & Pavía, 2014].

Regardless of the materials used in the construction of buildings, thermal conductivity is a very important property. A low value will help conserve heating or cooling energy and help keep the living environment at a comfortable temperature. There is greater effort nowadays in making buildings more eco-friendly. Lime render has been used as a finish to walls for a long time but the use of lime has gone through a renaissance due to its low embodied energy in production. It is used as a binder for hemp shiv and hemp fibres to create lime/hemp composites. Hemp straw

provides two products for building materials: hemp fibres are strong and can be used to make lime/hemp fibre panels and hemp shiv is used as a bio aggregate in hemp composites (also known as hemp concrete) [Collet & Prétot, 2014]. The lime/hemp shiv composite, in particular, has advantageous insulative characteristics as it has a low thermal conductivity (about 0.1 W/(m·K) minimum) [Bederina, Marmoret, Mezreb, Khenfer, Bali & Quéneudec, 2007] and is lightweight (density: 200-400 kg/m^3) [Amziane & Arnaud (Editors), 2013]. In addition, it has exemplary vapour permeability characteristics meaning the risk of condensation is greatly reduced [Brzyski, Barnat-Hunek, Suchorab & Łagód, 2017]

Following the Introduction in Section 1, the significance of this research is given in Section 2. A review of previous literature is presented in Section 3 and is used to identify and select the nanofillers and additives to be used to enhance the properties of lime based construction materials. The methodology used to determine the relevant properties of the materials are described in Section 4. The results with discussion are given in Section 5 followed by the application of the findings to a wall design in Section 6. The conclusions are given in Section 7.

2   Research Significance

Although hemp concrete has a low thermal conductivity of about 0.1 W/(m·K) as stated in Section 1, this is still much higher than current state-of-the art insulants such as vacuum insulation which has a thermal conductivity of only about 0.004 W/(m·K) [Alam & O'Flaherty, 2017]. It does not possess great strength characteristics so it is normally used with timber studding to enhance the structural performance. The paper will investigate ways of improving the thermal conductivity of lime render and lime/hemp composites with nanomaterials to create a high performing lime nanorender and hemp fibre/shiv nanocomposite. Since strength is an issue

4

for lime/hemp fibre composites (it was reported elsewhere that future research could focus on the use of additives to eliminate the wooden frame as the load-bearing structure of a wall [Barnat-Hunek, Smarzewski & Fic, 2015]), the influence of adding an environmentally friendly PVAc to the nanocomposite on compressive strength will also be investigated. The newly developed nanocomposite materials will be used to design a high performance, load bearing eco-friendly wall. This will consist of a central Core (see Figure 1) comprising lime/hemp fibre/nanomaterial/PVAc to provide the strength element, thereby reducing reliance on timber studding, two layers of lime/hemp shiv/nanomaterials for enhanced insulative purposes (Insulator on both faces of the Core, Figure 1) and a lime/nanomaterial nanocomposite render to provide an aesthetically pleasing appearance inside and out (Figure 1).

[Figure 1 near here]

A further barrier to using lime and hemp as building materials is that a large thickness of material is required to meet thermal transmission requirements (U Values) as required by the Building Regulations [HM Government, 2010]. A large thickness not only negatively impacts on the footprint of the building, but it also influences the drying time meaning shuttering has to remain in place for a longer period of time and, therefore, extends the construction time. Damp and cold weather periods further aggravates this issue. The research employed rapid drying of the samples as soon as was practically possible to determine if accelerated water removal is worth pursuing as a technique for on-site construction. A number of accelerated drying techniques were investigated by Alvarez et al. [Alvarez, Fernandez, Navarro-Blasco, Duran & Sirera, 2013] and among these was a solvent exchange method and freeze-drying which performed well. Due to the size of the samples in this work, the solvent exchange method was

chosen as the accelerated drying method. This was implemented five days after casting when the samples were considered strong enough for demoulding to take place. Further considerations for an on-site water removable technique are given in Section 5.6.

3. Previous Research

The following sections investigate the influence of various factors on the thermal and/or mechanical properties of lime/hemp composites. A summary is provided at the end culminating in a description of the optimised selection of nanomaterials to improve the performance of the lime/hemp composites.

3.1.   *Methods to improve thermal conductivity*

Thermal conductivity of lime/hemp composites is a property which has received a lot of recent attention in the literature. Hemp was used to manufacture insulation panels (hemp fibres alone) or as a construction material (hemp bast and concrete mix) [Benfratello, Capitano, Peri, Rizzo, Scaccianoce & Sorrentino, 2013]. Their research showed good insulative characteristics (values between 0.0899 and 0.1408 W/(m·K) were obtained). They also found that the size of hemp shiv is important, shives with a granulometry higher than 4 mm are too brittle. The maximum quantity must be no more than 30% and 40% for shiv size 2 and 4 mm respectively.

A previous study reported that pre-treating hemp shiv by immersing in a liquid of $Ca(OH)_2$ improved many properties. The fibres and shives were saturated in calcium ions ($Ca2^+$) for eight hours followed by washing in water. When mixed with a hydrated lime binder (by volume: 29% lime, 40% hemp and 31% water), a decrease in thermal conductivity was found, the lowest being 0.171 W/(m·K) for the treated hemp shiv (length: 1.94 mm) in comparison to 0.219 W/(m·K) for untreated shiv of the same length. The thermal conductivity increased when the shiv length

6

increased for both Ca(OH)$_2$ treated and untreated hemp shiv due to an increase in density [Cigasova, Stevulova, Terpakova, Sicakova & Junak, 2013].

3.2. *Influence of density on thermal conductivity*

Thermal conductivity of hemp composites is impacted by density [Collet & Prétot, 2014]. It was reported that variations to the density of an industrially produced spray applied hemp shiv concrete (0.5 hemp: binder ratio) had a larger impact on thermal conductivity compared to changes in the moisture content. It was found that when the density increased by two-thirds, the thermal conductivity increased by 54%. However, the same material exhibited an increase of only 15%-20% in thermal conductivity when the moisture content increased from a dry condition to 90% relative humidity [Collet & Prétot, 2014].

Lime and hemp for construction usage, as reported in another study [Elfordy, Lucas, Tancret, Scudeller & Goudet, 2008] also used a spray applied technique to deposit the material. The mechanical properties increased as a result of better compaction, as did density, leading to a higher thermal conductivity. Densities of 417, 475, 496 and 551 kg/m^3 gave thermal conductivities of 0.179, 0.421, 0.542 and 0.485 W/(m·K) respectively. A compromise must be found between thermal conductivity and mechanical properties for designing load bearing walls.

A direct relationship between thermal conductivity and density was also found elsewhere [Kiran, Nandanwar, Naidu & Rajulu, 2012]. The thermal conductivity of bamboo mat board was conducted at constant fixed temperatures of 30°C and 50°C and bulk densities of 0.75 to 1.65 g/cm^3. From a starting point of 0·121 W/(m·K) for bulk density of 0·765 g/cm^3, thermal conductivity increased to 0.384 W/(m·K) for a bulk density of 1.61 g/cm^3. Density and thermal

conductivity showed a linear relationship between them. From the results, the thermal conductivity of bamboo mat board increased with increasing bulk density.

An increase in density was also observed due to aluminium nanoparticles comprising different bulk densities pellets, the thermal conductivity increased from 0.2 W/(m·K) up to 1 W/(m·K) as densities increased from 1.1 to 2.3 g/cm^3 as a result of more contact between particles by consolidation [Stacy, Zhang, Pantoya & Weeks, 2014].

In other studies, it was found that the thermal conductivity decreased for hemp-lime to give comfortable thermal indoor conditions and low energy requirements. Adding 70 % of cork granulate to hydraulic lime with cement, the thermal conductivity decreased by 75 % for conventional cement mortar and 50 % for NHL5 compared to the reference value [Kinnane, McGranaghan, Walker, Pavia, Byrne & Robinson, 2015]. Adding cork to a cement mortar was also beneficial as it led to an elimination of temperature variation (higher thermal delay) and permeability decrease for the same starting temperature [Brás, Gonçalves & Faustino, 2014].

3.3. *Influence of nanomaterials on thermal conductivity*

There has been some work done on investigating the influence of nanomaterials on properties of hemp based materials. nZnO and nClay mixed in a wood polymer composite can increase the mechanical properties, thermal stability and ultraviolet resistance of the composites due to its behaviour as an ideal UV blocker and UV inorganic absorber [Hazarika & Magi, 2014]. The temperature propagation was largely reduced in a sono-chemically heated system by existence of ZnO nanofluid. The nanofluid zinc oxide at 4% dosage increased heat absorption capacity by about 30-40% [Bhagat, More & Khanna, 2015].

Furthermore, it was reported that after a cement paste was heated to 350⁰C and 900⁰C for six hours, the 28 day thermal conductivities of the cement paste mixed with 1-5% wt. $nSiO_2$ reduced by 38% (range: 0.42 - 0.57 W/(m·K)) after heating to 900 °C compared to the paste at ambient temperature [Jittabut, 2015]. The results after heating to 350ºC were very close to those obtained at ambient temperature.

An aerogel based plaster (nanotechnology coating) was found to have a higher potential of heat isolation meaning the required thickness of plaster can be reduced to yield the same thermal performance [Barbero, Dutto, Ferrua & Pereno, 2014]. A research paper reported that replacing ordinary Portland cement by 1% by weight of nClay improved thermal stability, reduced porosity and water absorption as it increased density, flexural strength, fracture toughness and impact strength of the hemp fabric-reinforced cement nanocomposite [Hakamy, Shaikh & Low, 2014]. However, adding more than 1 wt. % adversely affected thermal, physical and mechanical properties.

3.4. *Summary*

In the present work, $nSiO_2$ and nZnO were chosen as nanomaterials to study their effect on thermal conductivity of NHL5 lime binder or render. nClay was identified as the nanomaterial to improve the mechanical strength at around 2% loading but concerns existed as to its influence on thermal conductivity. $nSiO_2$ not only enhances the mechanical strength but also decreases porosity and shrinkage, loading 2% by weight of lime was suggested. Adding nZnO at 4% wt. lime is expected to decrease thermal conductivity with additional benefits such as stability and protection against UV effects.

The choice of organic materials was hemp shiv and hemp fibre mixed with lime binder to give a nanocomposite material (images of the hemp used are given in Figure 2). The length of the hemp fibres were in the range 6-12 mm and were cut manually using a scissors. Lime plus selected nanomaterials was chosen as the render. The aim is to develop high performing wall layers as shown in Figure 1. The tests conducted were dependant of the requirements of the various layers in Figure 1 and consisted of a mixture of thermal conductivity, porosity/density and compressive strength.

[Figure 2 near here]

4. Methodology

4.1. Materials

Singleton Birch Secil Natural Hydraulic Lime NHL 5 was purchased from Lincolnshire Lime in the UK. Nanomaterials (nClay, $nSiO_2$ and nZnO, selected on the basis of their beneficial properties as summarised in Section 3.4), were purchased from Sigma Aldrich in the UK. Hemp shiv was procured from East Yorkshire Hemp, Driffield, UK (average size: 15mm long x 5mm wide, thickness ~ 0.5mm). The hemp fibre was sourced from Wild Colours, Birmingham, UK. Polyvinyl acetate (PVAc) adhesive was purchased locally (Evo-Stik Super Evo-bond Waterproof PVA). A number of PVAc glues were available with similar claims about their properties but this one was chosen as it was marketed as an environmentally hazard-free wood glue.

For clarity, all percentages given with respect to hemp fibre and hemp shiv are their weight with respect to lime e.g. 30 % HS/Lime means 30 % of hemp shiv by weight of lime. With regards to % PVAc, it is the weight of adhesive by weight of water in the mixture.

4.2. Specimen preparation

A domestic mixer was used to mix the materials. The water lime ratio is 0.4 but since the nanofillers absorb water, this was accounted for by adding water to achieve a similar flow (150 mm) on a flow table compared to the control sample (in accordance with BS EN 1015-3, 1999). For complete nanomaterial dispersion, the nanomaterials were magnetically stirred in the water for two hours prior to adding to the mixture. nClay needed more stirring time for better dispersion so this continued overnight. The lime and hemp (shives or fibres) were dry mixed for five minutes. The PVAc was added to the water/nanomaterial mixture and stirred for 15 minutes before gradually pouring onto the dry mix of lime hemp (shives or fibres). Mixing continued for 5 minutes on slow speed and 10 minutes on quick speed. The mixed composite was then placed into a mould and compacted via tamping with a mallet of dimensions similar to the surface area of the specimen for compaction. Mould size of 180 x 130 x 20 mm was used for thermal conductivity and 40 x 40 x 160 mm for compressive and flexural strength.

At 5 days after casting, samples were carefully demoulded and immersed in isopropanol for 7 days. Following this, they were dried in an oven for two days at 60°C. At 14 days, samples were removed from the oven and either tested or transferred to a temperature control room (60% RH and 20°C).

4.3. Thermal conductivity

4.3.1 Apparatus

A procedure based on BS EN 12664 [BS EN 12664, 2001] was adopted for this work. This standard provides two methods, one of which (heat flow method) was used to conduct the tests reported in this paper. The test specimen is surrounded by a polystyrene isolator (insulation) and

a cold plate is used to reduce temperature on the underside of the specimen to 2⁰C. The upper

face is exposed to room temperature which is held fairly constant at about 16°C. Two

thermocouples are placed on each of the top and bottom faces of the specimen and averaged to

get the temperature gradient through the specimen. The specimens measuring 180 x 130 x 20mm

were cast in timber (wisaform) moulds. Two heat flux sensors (Hukseflux HFP01, 80mm

diameter, 5 mm thick) were placed on the warm face to obtain the heat flux through the specimen

as shown in Figure 3 with the average of both taken as the heat flux through the specimen.

[Figure 3 near here]

4.3.2   Theory

The simplified form of Fourier's Law was used to determine the one directional thermal

conductivity of the samples as follows:

$$q_x = -\lambda \, (dT/dx)$$

Equation 1

where

q_x is the heat flux in direction x (W/m^2)

λ is the thermal conductivity of the material (W/(m·K))

dT/dx is the thermal gradient in the direction of the flow (K/m)

The thermal conductivity of the samples was determined from the measured heat flux at steady

state conditions and the temperature difference between the hot and cold sides.

In order to assess the performance of the apparatus, the thermal conductivity of a 25 mm thick

sample of expanded polystrene (180 mm×130 mm) of known thermal conductivity (0.033

12

W/(m·K)) was used. Thermal conductivity of the reference polystrene sample was 0.032

W/(m·K), thereby proving that the apparatus can measure thermal conductivity of materials even

with very low λ with good accuracy [O'Flaherty & Alam, 2018]. Initially, two samples were

tested for the Control render and 30% Hemp shiv/lime which gave very good repeatability. One

sample was tested for all others. The test can last several hours until the temperature and heat

flux readings stabilise, hence it was considered that one sample was sufficient as all samples

followed a similar trend.

4.3.3   Test scenarios

A summary of the test scenarios is given in Table 1. Referring to Table 1 and Figure 1, the

samples investigated in the first series of tests (Render) consist of lime as the base material with

different nanomaterials added to determine their influence on thermal conductivity, λ.

Nanofillers used were None (i.e. control), $nSiO_2$, nZnO and nClay. The 'R' series of tests was

conducted first and the findings were used to formulate test series 'I' (Insulator) and 'C' (Core).

The second series "I" (Table 1) investigated the influence of selected nanomaterials on the

thermal conductivity of lime/hemp shiv, with and without PVAc since hemp shiv is known to

have very good insulative properties e.g. < 0.05 W/(m·K) (Kymäläinen & Sjöberg, 2008;

Schiavoni, Alessandro, Bianchi & Asdrubali, 2016). Nanofillers used in this series were None

(control), nZnO and nClay along with PVAc. The third series ('C', Figure 1) was devised to offer

strength to the wall hence hemp fibre and PVAc was used with lime and one nanomaterial for

this purpose.

[Table 1 near here]

With regards to the compressive strength testing for the 'C' specimen, Table 1, eight specimens were tested for strength and the average obtained. Apart from the compressive strength tests, one sample was tested for thermal conductivity and porosity as is generally the case for these test methods.

4.4. *Porosity and bulk density*

Mercury intrusion porosimetry was conducted on the Render samples to investigate the porous structure in a quantitative way. Porosity testing was not conducted on the specimens containing hemp shiv ('I') or hemp fibre ('C') due to their highly porous composition meaning porosity data may not be very useful (a study elsewhere found that the total porosity of hemp concretes ranged from 72% for precast hemp concrete to 85% for sprayed hemp concrete. The high porosity was due to a wide range of micrometric pores in the binder matrix and hemp shiv to millimetric pores due to the arrangement between the hemp shiv and to the hemp–binder adhesion, Collet & Prétot, 2014). Porosity of the 'R' samples was conducted at 60 days age i.e. 46 days stored at 20°C/60% RH upon completion of the solvent exchange drying technique at 14 days.

The volume of mercury that penetrates the specimens is recorded as a function of pressure [Aligizaki, 2006]. In particular, it can provide information on the pore size/volume distribution & specific surface (Section 5.3) and bulk density (Section 5.4) as these properties impact on aspects of material performance such as moisture movement, heat transfer and durability.

A mercury intrusion porosimeter PASCAL 140/240 was used which is capable of measuring pore size in the range of 116 μm to 0.0074 μm pore diameter. The test followed the procedures outlined in British Standard BS ISO 15901-1 [BS ISO 15901-1, 2016]. The test samples consisted of specimen fragments measuring approximately 5x5x10 mm, which were dried in a

fan-assisted oven at 60 ºC until constant weight prior to testing. The mercury contact angle was taken to be 140°.

4.5. *Compressive strength*

Compressive strength of the Core specimens (C, Figure 1) was determined using an Instron 3367, capacity 30 kN. The test was conducted in accordance with BS EN 1015-11, 1999. Compression strength was conducted on the two broken pieces from a flexural test, prism dimensions 160 x 40 x 40 mm. In order to determine the stress at failure, two small metal plates were placed above and below the specimen, dimension 40 x 40 x 5mm thick. A mid-range loading rate was used (30 N/s).

5. Results and Discussion

5.1. *Thermal conductivity*

An example of the thermal conductivity and mean temperature profiles versus time for a specimen (4% nZnO) is given in Figure 4. The thermal conductivity was obtained from the steady state portion of the graph (approximately from 30 mins onwards). This profile was similar for all specimens tested hence only the thermal conductivity values will be presented as described in Section 4.3.2.

[Figure 4 near here]

The results of the thermal conductivities are given in Table 2. Referring to Table 2, the wall layer (see Figure 1) is given in col. 1. The specimen ID is determined from Table 1 where the Test number (1-6) and nanofiller identifier (a-e) are combined to produce the identity (col. 2). The free water:lime ratio is given in col. 3 and is 0.4 for specimens in Test 1-3 but is either 0.75 or 0.9 for Test IDs 4-6 as hemp shiv or fibre is included in the mixture. The different ages at testing

is given in col. 4 and varies between 14 and 300 days. The quantity of nanofiller included as a percentage of the mass of lime is given in col. 5. The thermal conductivities, determined as described in Section 4.3 is given in col. 6, Table 2. From the data given in Table 2, a number of variables will be considered such as influence of nanofiller on thermal conductivity and porosity.

5.2. Influence of nanofiller on thermal conductivity

The thermal conductivities (λ) for the 'R' specimens (Table 2) are given in Figure 5. Thermal conductivities were determined at 14, 150 and 300 days age for the different specimens. At 14 days age, the best performing specimen was Specimen 1d consisting of 4% nZnO, λ being 0.131 W/(m·K). The Control averaged 0.159 W/(m·K), hence a reduction of 18%. Specimens 1b (2% nSiO2), 1c (2% nClay) and 1e (2% nClay+4% nZnO) also performed better than the control (0.154, 0.147 and 0.151 W/(m·K) respectively). Nanomaterial nZnO has high heat absorption capacity as shown elsewhere [Bhagat, More & Khanna (2015)] and this was the primary reason for Specimen 1b exhibiting the best performance. However, when 2% nClay was blended with 4% nZO, λ increased to 0.151 W/(m·K), higher than either Specimens c (2% nClay) and d (4% nZO). This is likely to be as a result of the higher bulk density due to the addition of nClay (see Section 5.4) as previous research [Hazarika & Magi, 2014] linked an increase in thermal conductivity to an increase in density.

The thermal conductivities at 150 days show an increase for Specimens 2a (Control), 2b (2% nSiO2) and 2c (2% nClay) but Specimen d (4% nZnO) maintains its low λ, now very marginally higher at 0.132 W/(m·K) compared to the 14 days value. A thermal conductivity test at 150 days for Specimen 2e was not conducted as the specimen got damaged prior to the test.

At 300 days, Specimen 3d (4% nZnO) exhibited a slight increase in λ to 0.147 W/(m·K) but still the lowest of all specimens. Specimen b (2% nSiO$_2$) exhibited the best thermal stability between 14 and 300 days with a relatively low thermal conductivity ranging between 0.152 to 0.160 W/(m·K). nClay exhibited the highest value at 300 days, λ being 0.201 W/(m·K). Despite an accelerated drying method being employed for all nanomaterials, λ increased over time, the highest increases were evident at 300 days. Further research is required to establish the reason behind this. It is likely that the storage conditions beyond the 14 days solvent exchange procedure had an influence. Specimens were stored under controlled conditions (20° C/60% RH) meaning the moisture content would have increased and likely leading to a higher λ. Furthermore, it is also possible that the hydration/carbonation process restarted. It could be due to reactions occurring as a result of certain nanomaterials. For example, a possible reason why the best performing nanorender (nZnO) increased its thermal conductivity is given elsewhere [Venkatesan, Khatiwada, Zhang & Qiao, 2015]. Although the research in question investigated the surface passivation of metal oxide for polymer solar cells, surface oxidation over time led to the nanomaterial becoming Zn metal which is higher in thermal conductivity than its oxide. Further research is needed to determine if oxidation is responsible for an increase in thermal conductivity in the lime/ZnO nanorender and establish ways to prevent it. The previous research suggested that surface oxidation can be suppressed by using a surface modifier like polyethyleneimine ethoxylated (PEIE).

[Figure 5 near here]

[Table 3 near here]

The thermal conductivities for the hemp shiv/lime nanocomposites ('Insulator') and hemp fibre/lime nanocomposite ('Core') are given in Figure 6. Specimen 4a is a Control sample and yields a λ of 0.098 W/(m·K). The best performing sample again includes 4% nZnO (Specimen 4d, 0.068 W/(m·K)) but as in the case of the renders (Figure 5), the blended nanofiller of 2% nClay and 4% nZnO produces a higher thermal conductivity (0.101 W/(m·K)), which is marginally higher than the control specimen. Specimen 5a which includes PVAc (30% wt. water) has a very similar λ to specimen 4d which includes the 4% nZnO (0.069 W/(m·K)). Since specimen 4d and 5a both possess similar λ values, other parameters such as strength and cost can be taken into account to establish which material best suits a particular purpose and this is briefly discussed in Section 5.5. The hemp fibre/lime nanocomposite ('Core') yielded a thermal conductivity of 0.122 W/(m·K), higher than the hemp shiv insulators but this is likely to be as a result of hemp fibres being used which have a greater influence on thermal conductivity than hemp shiv [Collet & Prétot, 2014]. Samples of insulators for strength testing were not made since the hemp shiv insulators were primarily designed as an insulator, not for strength. It will be shown in Section 5.5 that composites containing hemp shiv do not meet minimum strength requirements for load bearing walls.

 [Figure 6 near here]

5.3. *Influence of nanofiller on porosity*

The pore structure properties of the nano modified and Control renders are summarised in Table 3 and Figure 7. It is evident that all three nanomaterials affect the pore structure of the mortar by reducing the modal pore diameter d_{cr} and the porosity (Table 3). The highest porosity decrease was observed for the mortar modified with 4% nZnO (50.2% decrease compared to the Control),

followed by those modified with 2% nClay (13.2%) and 2% $nSiO_2$ (5.5%). The use of $nSiO_2$ yielded an increase in the total pore surface area of the mortar (Figure 7), which can be attributed to a reduction in the population of pores with diameters between 1 μm and 2 μm and an increase in the population of pores with diameters between 1 μm and 0.01 μm (Figure 8). A similar pore size distribution can be observed for the mortar modified with 2% nClay, however, this is characterised by a lower peak in the region of the modal pore diameter (≈ 0.9 μm) and by a smaller number of pores with diameters between 0.1 μm and 0.01 μm (Figure 8). This results in the mortar having a lower total pore surface area, close to that of the control. Whilst it yielded the biggest porosity decrease, the use of 4% nZnO had the lowest impact on the pore size distribution of the mortar, leading to a slight decrease in the modal pore diameter (Table 3). The observed porosity decrease is due to a reduction in the population of pores with diameters between 0.5 μm and 2 μm (Figure 8).

The results, therefore, have shown that the addition of nanomaterials has reduced both the porosity and thermal conductivity (Section 5.2) of the nanocomposites. This is not normally the case with building materials where a lower porosity is associated with a higher thermal conductivity. The specimen with the lowest thermal conductivity and lowest porosity (Figure 5-Figure 7) generally contained 4% nZnO. This nanomaterial has a high heat capacity and releases heat slowly as shown in Section 3.3, in addition to contributing to decreasing the pore size. However, further research would be beneficial on a larger number of samples with different recipes for all nanomaterials to fully confirm their thermal performance.

[Figure 7 near here]

[Figure 8 near here]

[Table 3 near here]

5.4. *Influence of nanofiller on density*

Bulk densities, ρ, of four of the lime renders are given in Figure 9 and were determined during the porosity testing (60 days age). The render with the lowest bulk density is Specimen d (4% nZnO) at 1.232 g/cm^3. Next best in the renders is Specimen b (2% nSiO2) at 1.261 g/cm^3 followed by the Control (1.339 g/cm^3) and Specimen c (2% nClay, 1.409 g/cm^3).

The longer term λ values (300 days age) are also given in Figure 9. Specimen d (4% nZnO) exhibits both the lowest density and lowest thermal conductivity. Specimens a and b also follow a similar trend but yield a higher ρ and higher λ compared to Specimen d. The nanorender specimen with the highest density also exhibits the highest λ and this was generally the case with other research findings as described in Section 3.2. The relationship between both properties for the lime nanocomposite renders in this research is shown in Figure 10. Referring to Figure 10, a linear relationship exists between λ and ρ which yield the equation

$$\lambda = 0.31\rho - 0.24$$

Equation 2

Therefore, it is clearly beneficial to design renders with lower bulk densities which will yield lower thermal conductivities.

[Figure 9 near here]

[Figure 10 near here]

5.5. *Compressive Strength*

In this research, the compressive strength of the Insulator (No's. 4, 5, Table 1) was not obtained as its main purpose is to provide insulative properties for the wall. However, previous research

20

has shown that the compressive strength of lime hemp shiv varied across a number of researchers. The highest compressive strength was 2.78 MPa [De Bruijn, Jeppsson, Sandin & Nilsson, 2009] whereas other researchers obtained strengths of 0.4-1.2 MPa [Arnaud, Cerezo & Samri, 2006] and 0.2-0.5 MPa [Evrard, 2003]. A load bearing lime/hemp material would require a compressive strength comparable to that of load-bearing lightweight expanded clay aggregate, i.e. 3-5 MPa [De Bruijn, Jeppsson, Sandin & Nilsson, 2009]. This is difficult to achieve with lime and hemp shiv alone, hence the reason for adding PVAc to the Core material containing lime and hemp fibres.

The average compressive strength of the Core material was 10.29 N/mm^2, 2-3 times stronger than the required strength to make it load bearing. There is, therefore, room to optimise the quantity of PVAc and other constituents in this material to make it more cost and thermally effective.

5.6. *Curing method*

The research reported in this paper showed that although the procedure adopted a water removal technique which stops the hydration process from the age of only 5 days, the tested materials still possessed the required characteristics of strength and thermal performance. More research is required to assess the influence of accelerated drying on the durability of renders and to investigate the best drying method for site use and the optimum time for implementation due to thickness of the material and possible adverse weather conditions. A possible candidate for site use would be microwave curing, a technique which has recently been developed at Sheffield Hallam University for accelerated curing of concrete patch repairs [Grigoriadis, Mangat & Abubakri, 2017; Mangat, Abubakri & Grigoriadis, 2017; Mangat, Grigoriadis & Abubakri, 2016] and has the potential to be used for site based accelerated drying.

6.   Applications of findings to wall design

Figure 1 provided a section through the proposed high performance wall to be designed with enhanced material properties from the findings presented in this paper. The new design consists of the five material layers as shown in Figure 11 (a) (numbered 2, 3, 4, 3, 2). For the purpose of U value calculations, Layer 1 is the external and internal air resistance. The design of the new eco-friendly wall will be compared to an existing design where conventional lime/hemp based materials are used, Figure 11 (b). Referring to Figure 11 (b), the wall consists of a lime/hemp mixture as the core of the wall with two layers of render on each face. Therefore, comparing Figure 11 (b) with Figure 11 (a), the lime/hemp core is extended to compensate for the insulator layers which have been omitted. Overall thickness remains the same. Additionally, the influence of the timber studding in Figure 11 (b) has been omitted for simplicity. Examples of Renders, Insulator and Core materials used in the project are given in Figure 12.

[Figure 11 near here]

[Figure 12 near here]

Table 4 shows the U value calculation for the new proposed design in Figure 11 (a). The Building Regulations [HM Government, 2010] state that a U value of 0.18 W/(m^2·K) is required for external walls to meet design requirements. Hence, the wall has been designed to comply with this requirement. It was assumed that the Render is 20 mm thick and the insulator layer is 100 mm thick. The thickness of the central core is then selected to achieve an overall U value of 0.18 W/(m^2·K), which for this design is 253mm. The overall thickness, therefore, is 493mm. For the purpose of calculations, the long term thermal conductivity for the Render was taken as the 300 day value, Table 2. The lowest thermal conductivity for the Insulator was 0.068 W/(m·K)

(Materials 4d, Table 2) whereas the thermal conductivity of the Core nanomaterial was taken as material 6d in Table 2. Referring to Table 4, the total thermal resistance of this wall is 5.55 m^2K/W giving the U value of 0.18 $W/(m^2 \cdot K)$.

[Table 4 near here]

If material 6d (λ=0.122 W/(m·K)) was replaced with the PVAc modified insulator containing hemp shiv as is commonly used in eco-friendly design (material 5a, Table 2, λ=0.069, assuming the minimum strength has been obtained through the addition of the PVAc), then the thickness of the core could reduce to 144 mm and still achieve a U value of 0.18 $W/(m^2 \cdot K)$. However, structural calculations would be required to ensure the wall is adequate to carry the applied loads. A similar calculation was conducted on an existing lime/hemp wall as shown in Table 5. The overall wall thickness is assumed as 493 mm to match the thickness of the wall design in Table 4. Again, two outer layers of render at 20 mm thickness is assumed, the remaining 453 mm consists of a lime/hemp shiv material (giving the total thickness of 493 mm). For the purpose of calculation, λ is taken as 0.098 W/(m·K) as obtained from the control material 4a in Table 2 (30% hemp shiv/lime). A slightly higher U value of 0.196 $W/(m^2 \cdot K)$ results (the thickness of this core would have to increase to 497 mm to comply with the Building Regulations U value of 0.18 $W/(m^2 \cdot K)$). Although there is not a great deal of difference between the new and existing wall design in terms of thermal conductivity and overall thickness, the major difference is the ability of the new wall design to be load bearing, hence eliminating the need to timber framing. However, research is required on the optimum constituents of the core material, either using hemp shiv or hemp fibre, to optimise the strength and thermal conductivities for enhanced performance. In addition, further research is also required on the most efficient method of

application, the options being site cast (leading to formwork requirements and drying issues as mentioned earlier) or as prefabricated blocks or panels installed using conventional techniques. Finally, it should be noted that excessive shrinkage could lead to cracking of the render. Possible solutions are to include a fine aggregate in the mixture or perhaps consider the inclusion of hemp fibre as a means of controlling shrinkage. However, further research is required to confirm this.

[Table 5 near here]

7. Conclusions

This study is conducted to investigate the influence of nanomaterials on the thermal characteristics of lime and hemp/lime composites for optimal wall design. An accelerated drying process was also trialled to assess its suitability in quickening drying times but without negatively influencing material properties. Based on the results from this experimental research, the following conclusions have been drawn:

- application of 4% nZnO to the lime render led to the lowest thermal conductivity. λ reduced by 18% to 0.131 W/(m·K) at 14 days compared to the Control sample (0.159 W/(m·K)). λ increased to 0.147 W/(m·K) at 300 days for this nanomaterial. Application of 2% $nSiO_2$ also helps reduce λ but not to the same extent as nZnO. The storage condition (60% RH) beyond the end of the solvent exchange procedure is likely to have influenced the longer term thermal conductivity.

- application of 4% nZnO to a 30% wt. hemp shiv/lime nanocomposite reduced the thermal conductivity by 31% compared to the control sample.

- the addition of the nanomaterials to the lime render had an impact on the density and thermal conductivity. Nanomaterial such as nClay led to a higher density than the control but nZnO

24

and nSiO$_2$ both exhibited lower densities and lower thermal conductivities. A linear relationship between thermal conductivity (λ) and bulk density (ρ) was determined where

$\lambda= 0.31\rho - 0.24$

- the render with 4% nZnO exhibited the lowest porosity (18.09%) whereas the renders with 2% nClay and 2% nSiO$_2$ both had porosities at 31.54% and 34.34% respectively. The Control specimen had a porosity of 36.35%. The 4% nZnO render specimen also exhibited the lowest total pore surface area of 0.592 m^2/g.

- two insulators exhibited similar thermal conductivity values hence selection of the optimum material should be based on not only thermal characteristics but also on cost and whether or not a stronger insulator is required to either share the load carrying with the hemp fibre core material or even replace it due to its lower thermal conductivity characteristics

- the core material consisting of 10% Hemp fibre/lime/30% PVAc/w and 4% nZnO exhibited an average compressive strength of 10.29 N/mm^2 so further optimisation is required for efficient structural and thermal performance.

- despite the application of the solvent exchange method at five days after casting, all nanocomposites still exhibited usable properties from the point of view of wall design. Further research is required to optimise an accelerated drying technique for site use.

The present study is based on investigating the influence of nanomaterials on the relevant properties required for hemp/lime construction. The study focused on improving the properties responsible for energy efficiency. The impact of the stronger core nanocomposite and insulator on the quantity of timber studding for strength is beyond the scope of this paper and will be considered in a future publication.

Word count: 6,848

References

Alam, M, & O'Flaherty, F. (2017), Thermal characterisation of Composite Insulation Panels using a vacuum insulated core, SOLARIS Conference 2017, Brunel University London, 27-28 Jul

Aligizaki, K.K. (2006). Pore structure of cement-based materials, Testing, interpretation and requirements, Modern Concrete Technology 12, CRC Press, ISBN 0-419-22800-4

Alvarez, J.I., Fernandez, J.M., Navarro-Blasco, I., Duran, A., & Sirera, R. (2013). Microstructural consequences of nanosilica addition on aerial lime binding materials: Influence of different drying conditions, Materials Characterization, vol. 80, June 2013, pp 36-49. https://doi.org/10.1016/j.matchar.2013.03.006

Arnaud, L., Cerezo, V., & Samri, D. (2006). Global approach for the design of building material containing lime and vegetable particles. In: The Sixth International Symposium on Cement and Concrete, Xi'an, pp. 1261–1265.

Barbero, S., Dutto, M, Ferrua, C, & Pereno, A. (2014). Analysis on existent thermal insulating plasters towards innovative applications: Evaluation methodology for a real cost-performance comparison, Energy and Buildings, vol. 77, pp. 40-47. https://doi.org/10.1016/j.enbuild.2014.03.037

Barnat-Hunek, D. , Smarzewski, P., Fic, S. (2015). Mechanical and thermal properties of hemp-lime composites, Composites Theory and Practice, 15, 1, 21--27.

Bederina, M., Marmoret, L., Mezreb, K., Khenfer, M.M., Bali, A., & Quéneudec, M. (2007). Effect of the addition of wood shavings on thermal conductivity of sand concretes: experimental study and modelling. Constr Build Mater; 21:662–8. https://doi.org/10.1016/j.conbuildmat.2005.12.008

BEIS, 2018. Department for Business, Energy and Industrial Strategy. Energy Consumption in the UK July 2018. https://assets.publishing.service.gov.uk/government/uploads/system/uploads/attachment_data/file/729317/Energy_Consumption_in_the_UK__ECUK__2018.pdf (accessed 16 Oct 2018)

Benfratello, S., Capitano. C., Peri, G., Rizzo, G., Scaccianoce, G., & Sorrentino, G. (2013), Thermal and structural properties of a hemp–lime biocomposite, Construction and Building Materials, vol. 48, pp. 745-754, 11. https://doi.org/10.1016/j.conbuildmat.2013.07.096

Bhagat. U.K., More. P.V., & Khanna, P.K. (2015) Study of Zinc Oxide Nanofluids for Heat Transfer Application. SAJ Nanosci Nanotech 1: 101

Brzyski. P., Barnat-Hunek. D., Suchorab. Z., & Łagód. G. (2017), Composite Materials Based on Hemp and Flax for Low-Energy Buildings, Materials, 10, 510; doi:10.3390/ma10050510

Amziane, S., & Arnaud, L. (Editors) (2013). Bio-aggregate-based Building Materials, Applications to Hemp Concrete. ISTE Ltd and John Wiley & Sons Inc; 2013. ISBN: 978-1-848-21404-0

Brás, A., Gonçalves, F., & Faustino, P. (2014). Cork-based mortars for thermal bridges correction in a dwelling: Thermal performance and cost evaluation, Energy and Buildings, vol. 72, pp. 296-308, 4. https://doi.org/10.1016/j.enbuild.2013.12.022

BRE 2015. The cost of poor housing in the European Union, Simon Nicol, Mike Roys, David Ormandy and Veronique Ezratty, www.bre.co.uk/filelibrary/Briefing%20papers/92993_BRE_Poor-Housing_in_-Europe.pdf. (accessed 16 Oct 2018)

BS EN 1015-3:1999 Methods of test for mortar for masonry — Part 3: Determination of consistence of fresh mortar (by flow table). ISBN 0 580 30746 8, 15 June 1999, amended January 2007

BS EN 1015-11:1999 Methods of test for mortar for masonry — Part 11: Determination of flexural and compressive strength of hardened mortar. ISBN 0 580 35469 5, 15 November 1999, amended January 2007

BS EN 12664:2001. Thermal Performance of Building Materials and Products–Determination of Thermal Resistance by Means of Guarded Hot Plate and Heat Flow Meter Methods–Dry and Moist Products of Medium and Low Thermal Resistance. (2001).

BS ISO 15901-1 (2016). Evaluation of pore size distribution and porosity of solid materials by mercury porosimetry and gas adsorption. Mercury porosimetry

Cigasova, J., Stevulova, N., Terpakova, E., Sicakova, A., & Junak. J. (2013), Modified hemp hurds as a filler in composites, International Multidisciplinary Scientific GeoConference: SGEM: Surveying Geology & mining Ecology Management, p. 385.

Collet, F., & Prétot, S. (2014), Thermal conductivity of hemp concretes: Variation with formulation, density and water content, Constr Build Mats, vol. 65, pp. 612-619. https://doi.org/10.1016/j.conbuildmat.2014.05.039

Committee on Climate Change, 2008. UK regulations: the Climate Change Act. www.theccc.org.uk/tackling-climate-change/the-legal-landscape/global-action-on-climate-change/ (accessed 16 Oct 2018)

De Bruijn, P.B., Jeppsson, K.H., Sandin, K, & Nilsson, C. (2009), Mechanical properties of lime–hemp concrete containing shives and fibres. Biosystems engineering, 2009. 103(4): p. 474-479. https://doi.org/10.1016/j.biosystemseng.2009.02.005

Elfordy, S., Lucas, F., Tancret, F., Scudeller, Y., & Goudet, L. (2008), Mechanical and thermal properties of lime and hemp concrete ("hempcrete") manufactured by a projection process, Constr Build Mats, vol. 22, pp. 2116-2123. https://doi.org/10.1016/j.conbuildmat.2007.07.016

Evrard, A. (ed.) (2003). Betons de Chanvre, Synthese des proprietes physiques [Hemp Concretes, a Synthesis of Physical Properties]. Report. Construire en Chanvre, Saint Vale rien (in French).

Grigoriadis, K., Mangat. P.S., & Abubakri, S. (2017), Bond between microwave cured repair and concrete substrate Mater Struct 50: 125. https://doi.org/10.1617/s11527-016-0990-6

Hakamy, A., Shaikh, F., & Low, I. M. (2014). Thermal and mechanical properties of hemp fabric-reinforced nanoclay–cement nanocomposites, Journal of Materials Science, vol. 49, pp. 1684-1694. https://doi.org/10.1007/s10853-013-7853-0

Hazarika, A., & Magi. T.K. (2014), Modification of Softwood by Monomers and Nanofillers. Defence Science Journal, [S.l.], v. 64, n. 3, p. 262-272, ISSN 0976464X. Available at: http://publications.drdo.gov.in/ojs/index.php/dsj/article/view/7325/4034>. doi:http://dx.doi.org/10.14429/dsj.64.7325. Date accessed: 16 Oct 2018.

HM Government, The Building Regulations 2010, Conservation of fuel and power, Approved Document L1A, 2013 Edition incorporating 2016 amendments - for use in England. https://assets.publishing.service.gov.uk/government/uploads/system/uploads/attachment_data/file/540326/BR_PDF_AD__L1A__2013_with_2016_amendments.pdf. Accessed 18 Oct 2018

Jittabut, P. (2015), Effect of Nanosilica on Mechanical and Thermal Properties of Cement Composites for Thermal Energy Storage Materials, Energy Procedia, vol. 79, pp. 10-17. https://doi.org/10.1016/j.egypro.2015.11.454

Kinnane, O., McGranaghan, G., Walker, R., Pavia, S., Byrne, G., & Robinson, A. (2015). Experimental investigation of thermal inertia properties in hemp-lime concrete walls Proceedings of the 10th conference on advanced building skins, Bern, Switzerland, pp. 942-949.

Kiran, M., Nandanwar, A., Naidu, M.V., & Rajulu, K.C.V. (2012), Effect of density on thermal conductivity of bamboo mat board, International Journal of Agriculture and Forestry, vol. 2, pp. 257-261. DOI: 10.5923/j.ijaf.20120205.09

Kymäläinen, H.R. & Sjöberg, A.M. (2008). Flax and hemp fibres as raw materials for thermal insulations, Building and Environment, 43, 7, 1261-1269. https://doi.org/10.1016/j.buildenv.2007.03.006

Mangat, P & Ojedokun O (2018). Pore size distribution of an alkali activated cementitious (AACM) mortar. Influence of curing on pore properties and strength of alkali activated mortars. Construction and Building Materials, 188, 337-348, https://doi.org/10.1016/j.conbuildmat.2018.07.180

Mangat, P.S., Abubakri, S., & Grigoriadis, K. (2017), Bond of steel reinforcement with microwave cured concrete repair mortars, Mater Struct 50: 249. https://doi.org/10.1617/s11527-017-1115-6

Mangat, P., Grigoriadis, K., & Abubakri, S. (2016). Microwave curing parameters of in-situ concrete repairs. Constr Build Mats, 112, 856-866. https://doi.org/10.1016/j.conbuildmat.2016.03.007

O'Flaherty, F., & Alam, M. (2018). Thermal and sound insulation performance assessment of vacuum insulated composite insulation panels for building façades, Advances in Building Energy Research, DOI: 10.1080/17512549.2018.1520645

Schiavoni, S., Alessandro, F.D., Bianchi, F. & Asdrubali, F. (2016). Insulation materials for the building sector: A review and comparative analysis, Renewable and Sustainable Energy Reviews, 62, 988-1011. https://doi.org/10.1016/j.rser.2016.05.045

Stacy, S.C., Zhang, X., Pantoya, M., & Weeks, B. (2014), The effects of density on thermal conductivity and absorption coefficient for consolidated aluminum nanoparticles, International Journal of Heat and Mass Transfer, vol. 73, pp. 595-599, 6. https://doi.org/10.1016/j.ijheatmasstransfer.2014.02.050

Venkatesan, S., Khatiwada, D., Zhang, C., & Qiao, C. (2015). Enhanced Lifetime of Polymer Solar Cells by Surface Passivation of Metal Oxide Buffer Layers. ACS Applied Materials & Interfaces, 2015. 7(29): p. 16093-16100. DOI: 10.1021/acsami.5b04687

Walker R & Pavía S, Moisture transfer and thermal properties of hemp–lime concretes. Construction and Building Materials, 2014. 64: p. 270-276, https://doi.org/10.1016/j.conbuildmat.2014.04.081
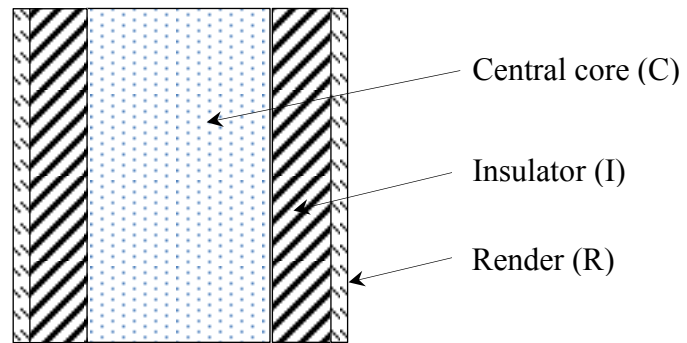
Figure 1 Cross section through wall: (R) Lime nanocomposite render; (I) lime/hemp shiv nanocomposite insulator (C); lime/hemp fibres nanocomposite.

(a)   (b)   (c)

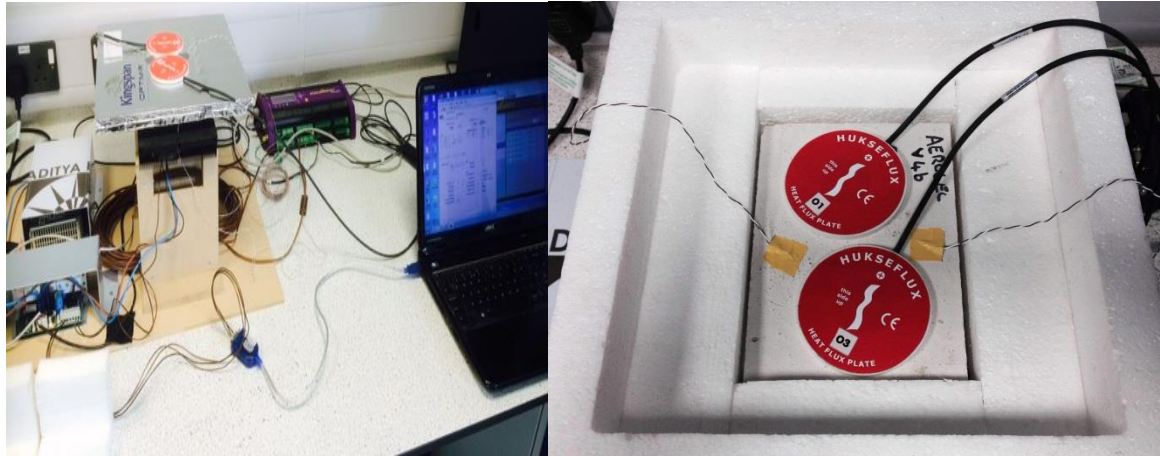**Figure 2** Hemp used in the specimens: (a) hemp fibre, uncut; (b) hemp fibre, cut; (c) hemp shiv

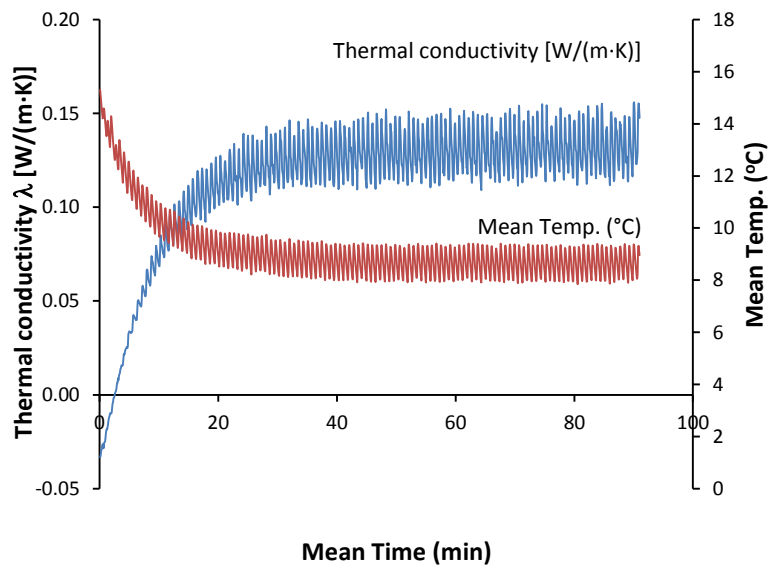**Figure 3** Heat flow meter device (left) with specimen under test (right)

Mean Time (min)

Figure 4 Determination of thermal conductivity for a Render (R) specimen (4% nZnO)
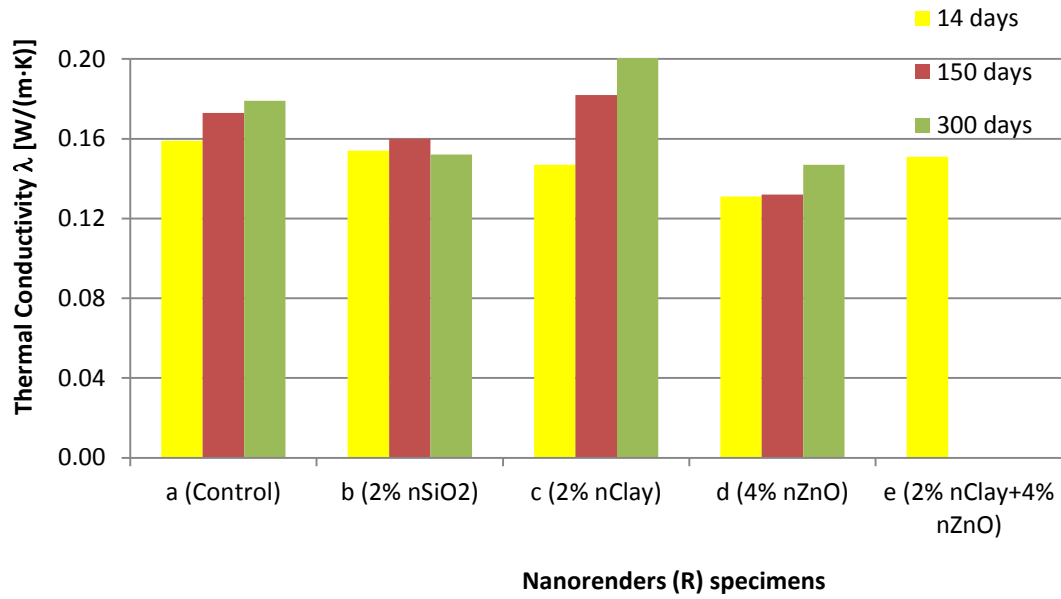
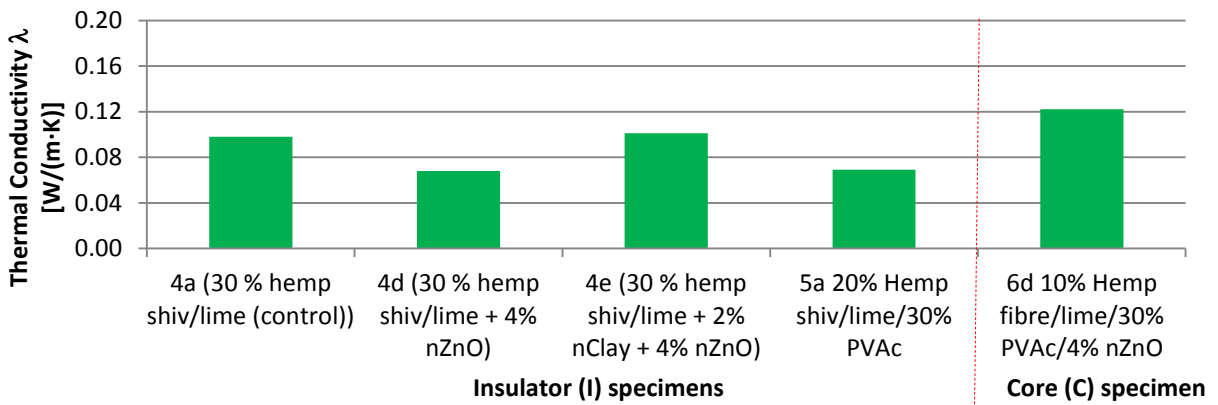**Figure 5** Influence on nanofiller and age on thermal conductivity for lime specimens (Renders, R)

Figure 6 Influence on nanofiller on thermal conductivity for hemp shiv or fibre/lime nanocomposites
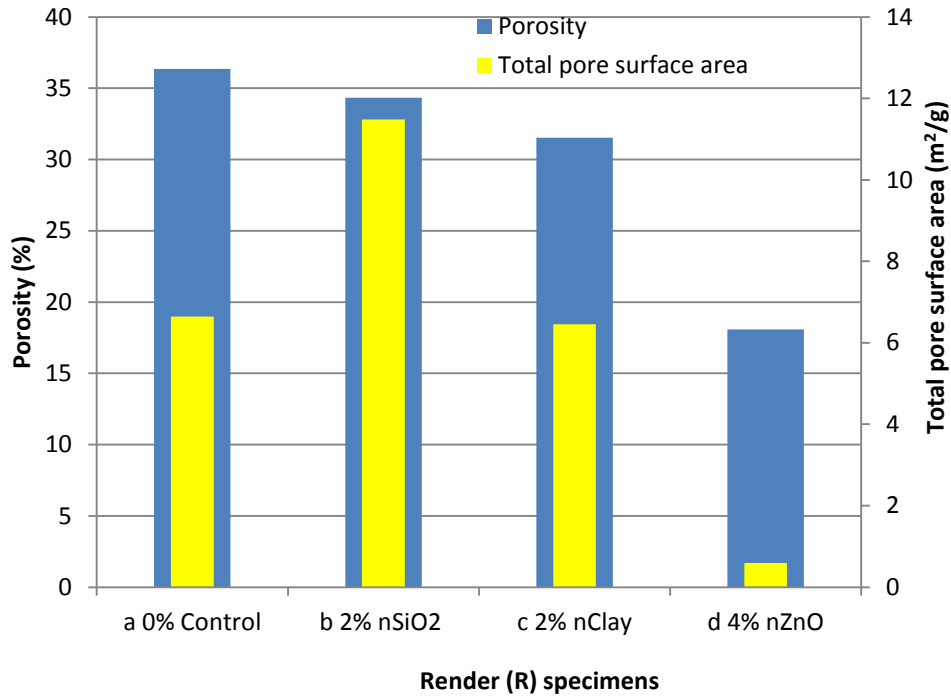
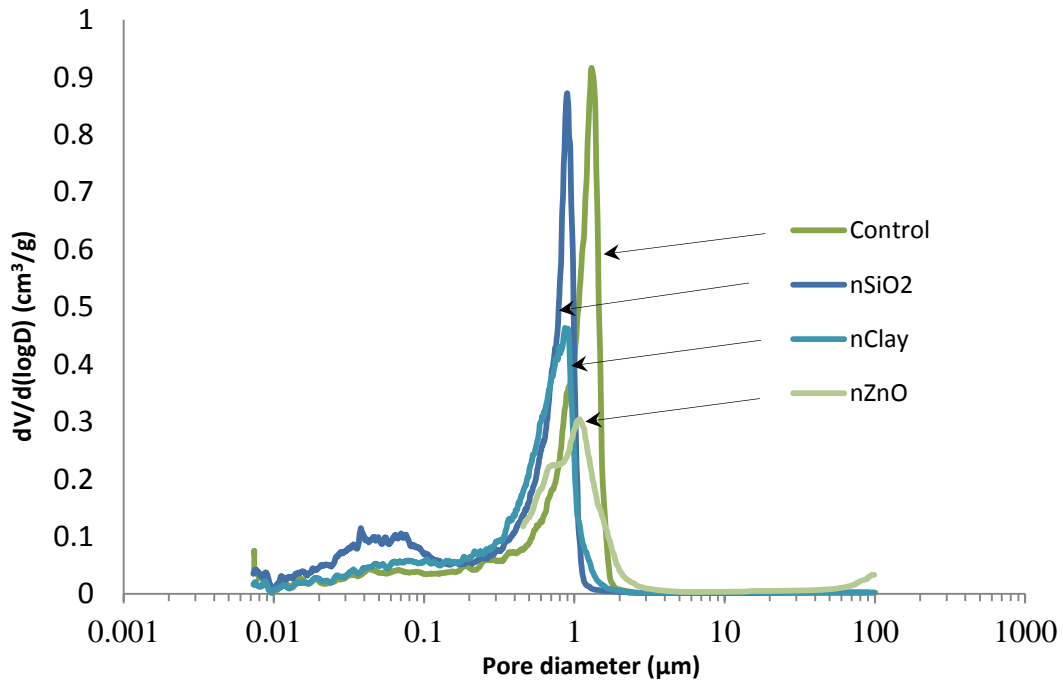**Figure 7** Comparison of total porosity and total pore surface area of Render (R) specimens

Figure 8 Differential volume of intruded mercury versus pore diameter of modified and control nanorender (R) samples
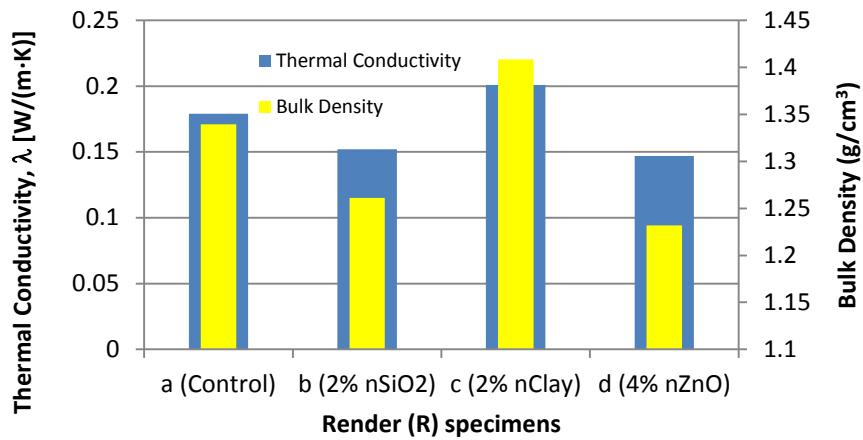
Figure 9 Bulk density and thermal conductivity of 'R' specimens
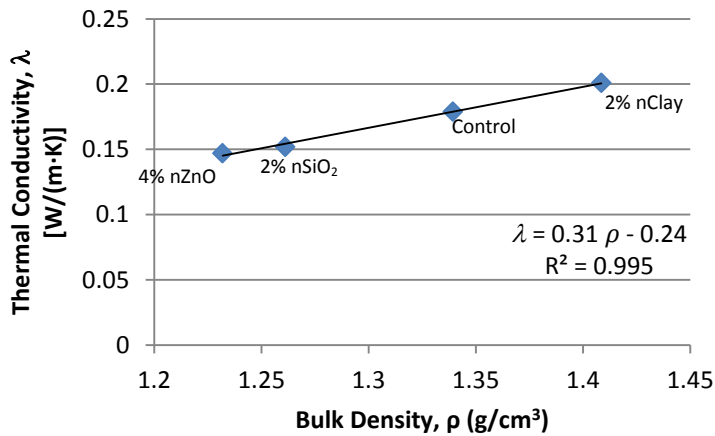

Figure 10 Relationship between bulk density and thermal conductivity for lime nanocomposite renders (R)
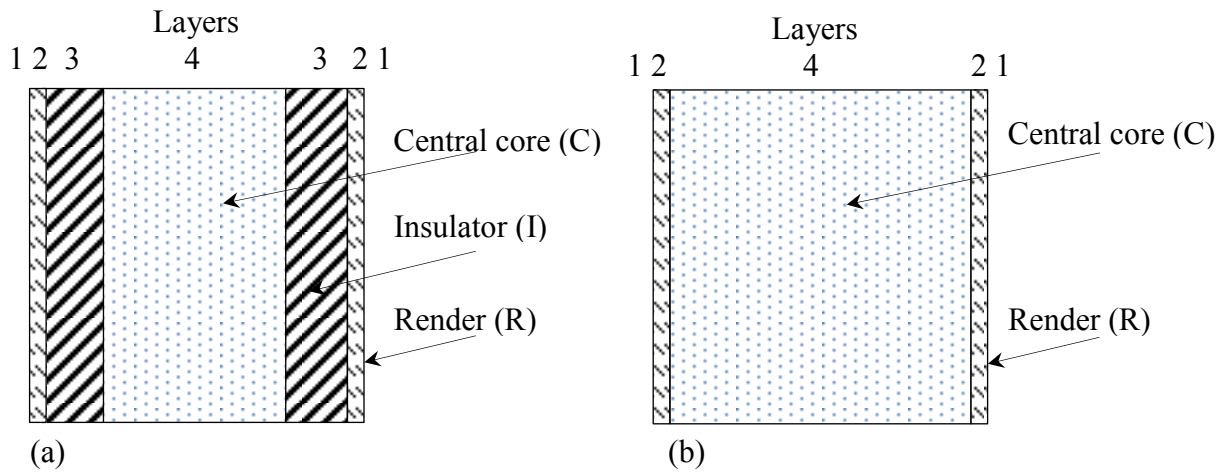
Figure 11 Cross section through: (a) eco-friendly wall; (b) lime/hemp wall (timber studding omitted for clarity)
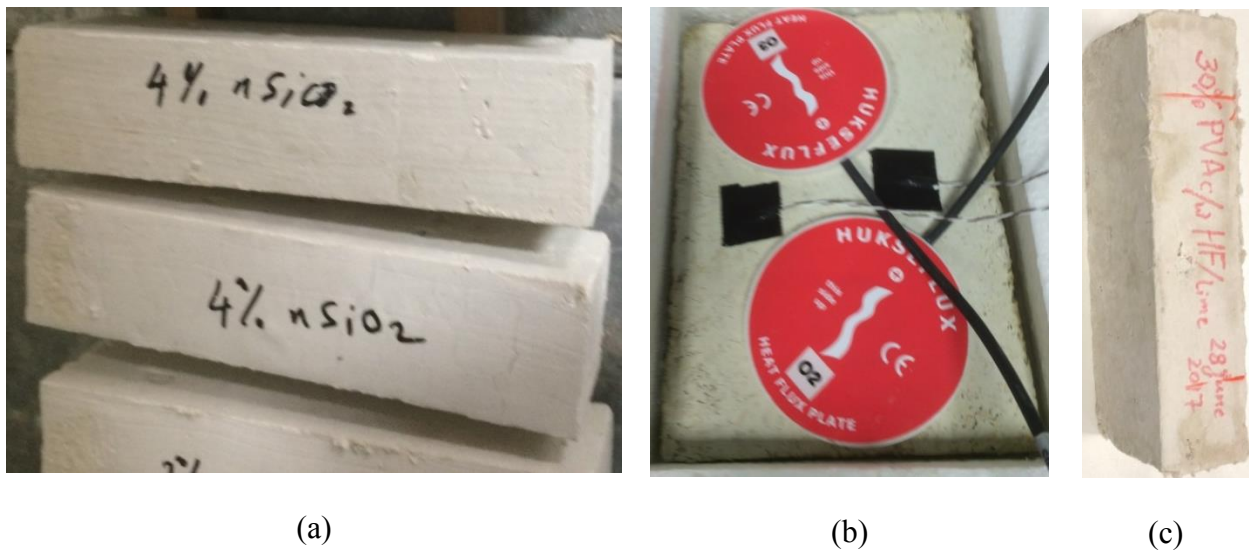

Figure 12 Examples of (a) Renders, R; (b) Insulator, I and (c) Core, C

Tables

Table 1 Test Schedule for thermal conductivity, porosity and compressive strength

Part*	No	Base material	W/L ratio	Age at test (days)+	Nanofillers (% by wt lime)				
					a	b	c	d	e
					Control	nSiO$_2$	nClay	nZnO	nZnO + nClay
R	1	Lime	0.4	14	**None**	**2%**	**2%**	**4%**	4%+2%
	2	Lime	0.4	150	None	2%	2%	4%	-
	3	Lime	0.4	300	None	2%	2%	4%	4%+2%
I	4	30% Hemp shiv/lime	0.75	14	None	-	-	4%	4%+2%
	5	20% Hemp shiv/lime/30% PVAc/water	0.75	14	None	-	-	-	-
C	6	10% Hemp fibre/lime/30% PVAc/water	0.75	14	-	-	-	**4%**	-

*R = Render; I = Insulator; C = Core, see Figure 1

+ Specimens demoulded at 5 days, immersed in isopropanol for 7 days, oven dried at 60°C for 2 days (14 days total). Stored beyond 14 days at 20°C/60% RH

Render samples 1a, 1b, 1c, 1d (highlighted in Bold) tested for porosity. Core sample 6d (highlighted in Bold) tested for compressive strength

Table 2 Thermal conductivity test results

1	2	3	4	5	6
Part*	**ID**	**W/L ratio**	**Age at test (days)+**	**% Nanofiller/Lime**	**Thermal conductivity [W/(m·K)]**
	1a	0.4	14	0% (control)	0.159
	1b	0.4	14	2% nSiO$_2$	0.154
	1c	0.4	14	2% nClay	0.147
	1d	0.4	14	4% nZnO	0.131
	1e	0.4	14	4% nZnO + 2% nClay	0.151
	2a	0.4	150	0% (control)	0.173
R	2b	0.4	150	2% nSiO$_2$	0.160
	2c	0.4	150	2% nClay	0.182
	2d	0.4	150	4% nZnO	0.132
	3a	0.4	300	0% (control)	0.179
	3b	0.4	300	2% nSiO$_2$	0.152
	3c	0.4	300	2% nClay	0.201
	3d	0.4	300	4% nZnO	0.147
	4a	0.75	14	30 % hemp shiv/lime (control)	0.098
	4d	0.9	14	30 % hemp shiv/lime/4% nZnO	0.068
I	4e	0.75	14	30 % hemp shiv/lime/4% nZnO/2% nClay	0.101
	5a	0.75	14	20% Hemp shiv/lime/30% PVAc	0.069
C	6d	0.75	14	10% Hemp fibre/lime/30% PVAc/4% nZnO	0.122

*R = Render; I = Insulator; C = Core, see Figure 1

+ Specimens demoulded at 5 days, immersed in isopropanol for 7 days, oven dried at 60°C for 2 days (14 days total). Stored beyond 14 days at 20°C/60% RH

Table 3 Pore structure properties

Part	Specimen	Porosity (%)	Porosity decrease (%)	d_{cr} (µm)	Total pore surface area (m²/g)
	a Control	36.35	-	1.301	6.647
R	b 2% nSiO₂	34.34	5.5	0.8958	11.482
	c 2% nClay	31.54	13.2	0.8645	6.451
	d 4% nZnO	18.09	50.2	1.088	0.592

Table 4 Design of new wall with nanocomposite materials

Layer	Materials	λ [W/(m·K)]	Thickness (m)	R [m²K/W]	U [W/(m²·K)]
1	External Resistance	-	-	0.13	
2	Render (lime nanocomposite)	0.147	0.02	0.14	
3	Insulator (lime/hemp shiv PVAc)	0.068	0.1	1.47	
4	Core (lime/hemp fibres)	0.122	0.253	2.07	
5	Insulator (lime/hemp shiv PVAc)	0.068	0.1	1.47	
6	Render (lime nanocomposite)	0.147	0.02	0.14	
7	Internal surface resistance	-	-	0.13	
			0.493	5.55	0.180

Table 5 Design of lime/hemp wall without nanocomposites

Layer	Materials	λ [W/(m·K)]	Thickness (m)	R [(m²·K)/W]	U [W/m²·K]
1	External Resistance	-	-	0.13	
2	Lime render	0.179	0.02	0.11	
3	-				
4	Lime/hemp shiv	0.098	0.453	4.62	
5	-				
6	Lime render	0.179	0.02	0.11	
7	Internal Resistance	-	-	0.13	
			0.490	5.08	0.196